JCPT

Small-Diameter Gas Lift Systems—A Potential Technical Solution for Transport of Fluids From Low-Pressure Reservoirs

J. BECARIA*
University of Alberta
* Presently with EnCana Corporation

P. TOMA
P.R. Toma Consulting Ltd.

E. KURU
University of Alberta

Abstract

Continuous or intermittent artificial lifting technology is competing today with electrical submersible progressive cavity (PC) pumping and sucker rod pumping for producing fluids from low-pressure reservoirs. If the shut-in fluid level is less than 45% of the depth of the well, finding a suitable and economic artificial lifting technology is a challenging task.

There are thousands of dormant gas wells where bottom water accumulations of 50 m or less impede gas production. Similar conditions are often found in coalbed methane reservoirs. Due to variable (and shallow) water levels and gas presence, rod pumping cannot be used and submersible electric pumps often pose operational problems. Depending on local conditions and economics, gas lifting, alone or associated with other artificial lifting technologies, can be used for producing such reservoirs. Within a limited range of gas-liquid flow rates, depth, and reservoir pressure, the use of small-diameter pipes for gas lifting technology can become a viable technology.

Laboratory investigations dedicated to small-diameter gas lifting operations have been so far limited to fluid transfer operations requiring a maximum of 10 – 20 m. This study uses mechanistic modelling approaches to respond to the industry's need for a better evaluation of depth/diameter flow rate limitations in view of assessing potential field applications of gas lifting for low reservoir pressures and relatively small liquid flow rates.

Laboratory tests were conducted in a specially designed rig. Experimental results were used to evaluate the accuracy of the existing model predictions and for assessing the effect of injected gas flow rates, reservoir pressure, and liquid interfacial tension on the liquid production rates.

To improve predictions of existing mechanistic models, particularly for small-diameter tubings and low pressure reservoir conditions, a new model is proposed and compared first with experimental results. The new model is then used as a scaling tool for assessing critical field depth conditions.

Introduction

Gas lifting or air lift has been used to remove water from flooded mines since 1782[1, 2]. Today, natural gas lifting is commonly used for oil wells where gas and liquid are produced together.

Conventional gas lifting uses tubing (or ducts) with a diameter greater than 2.54 cm. Vertical upward transport of gas and liquid for such conditions is well investigated and both empirical[3] and mechanistic models are available[4-6].

During the last 20 years, mechanistic models are gaining more acceptance, replacing empirical models. Development of a mechanistic model involves: a) extensive visual observations of field and laboratory-scale models in view of assessing specific boundaries of flow patterns (e.g., bubble, slug, annular, stratified, etc.); b) assessment of the main gas-liquid features (e.g., bubbles, liquid film, etc.) and of the phases interface aspect (e.g., smooth, wavy, etc); c) estimation of local gas and liquid velocities, including the slip; d) estimations of local void fraction and of static and dynamic pressures; e) computer-assisted integration of "local" features to include the pipe pressure-volume-temperature (axial) profile; and, f) field validation.

Flow pattern mapping and the drift-flux model[7] are essential tools used to evaluate the gas-liquid relative velocities and local void fraction. For a certain gas injected and specific gas-liquid properties, the liquid reservoir production is obtained at the cross-section between the bottomhole pressure-production curve (IPR) and the vertical lift performance (VLP—indicating the bottomhole pressure for a given gas-liquid rate and tubing geometry). For conventional gas lifting operations, the static pressure is often much greater than the dynamic (frictional) one. Efforts are continuously made to reduce the static pressure component and increase production through properly designed gas-lifting operations.

The gas-liquid flow in long small-diameter pipes (SDP) for upward transport of relatively small liquid rates under low reservoir pressure conditions is still un-mapped territory. One of the most common flow patterns encountered with gas lifting operations—the slug flow—indicates a certain increase of the void fraction with decreasing the pipe diameter. The potential reduction of static pressure with SDP is investigated in this study, particularly for gas lifting applications with low-pressure reservoirs and limited liquid-gas flowrates. However, when the pipe diameter is further reduced, for the same gas-liquid transport conditions, frictional pressure drop becomes important and the advantage offered by SDP is lost.

The liquid film downflow, observed for all gas lift operating as slug flow pattern, is assumed to be negligible when compared with the amount of liquid transported upward. However, for SDP, the liquid fallback condition can essentially limit the depth of net upward liquid transportation. This aspect is given special consideration in this study. An improved model for the calculation of maximum transportation depth as a function of reservoir pressure, gas injection, and liquid properties is validated for laboratory conditions and used to assess limiting field conditions.

Conventional gas lifting has been used extensively in the past[2] to increase reservoir liquid production through the significant reduction of the static pressure component. More recently, gas lifting was extended to produce from low-pressure reservoirs (stripper wells) and enhance waterflood operations[8]. Past experience[8] indicated that gas lifting applied to reservoirs with less than 50% submergence is not always successful and additional numerical models would be required to reduce the operational risk.

PEER REVIEWED PAPER ("REVIEW AND PUBLICATION PROCESS" CAN BE FOUND ON OUR WEB SITE)

Local Pressures and Vertical Lift Performance Curve

For situations where compressed gas is injected from the surface, the point of gas injection and the gas injection rate are essential to determine and optimize the production rate (obtained as the cross-section of measured IPR and calculated VLP). The numerical solution is obtained by simply balancing the measured BHP (IPR curve) with the calculated BHP (for certain gas-liquid flowrates). The sum of static and frictional pressure drops is calculated for a certain tube diameter D, and gas and liquid flow rates [Equation (1)] to obtain the vertical lift performance curve (VLP):

$$P_{res} = \sum_{i=1}^{n} \left(dP_{fr} + dP_{st} \right)_{D,Q_G,Q_L} + P_{WH} \quad \text{..... (1)}$$

The total depth (length) of the well is divided into n sections. For each section, the entrance pressure and temperature, $(P,T)_{in}$, are considered constant. The calculated exit pressure and temperature, $(P,T)_{ex}$, are used as entrance values for the next section.

Accurate estimation of static pressure drop requires a good knowledge of actual gas-liquid velocities, essential for estimating the local void fraction (α) and gas-liquid density. Actual gas/liquid velocities depend on total transport velocity and on the phase slip velocity. Equation (2a) is a simplified version of the drift-flux model[7] where the value of local gas velocity U_G is a function of transport velocity U_m [Equation (2b)] and the gas distribution coefficient c. While the transport velocity U_m is calculated with the known/assumed gas-liquid local flowrates, the terminal velocity (u_t) depends on the type of gas bubble and local flow pattern:

$$U_G = cU_m + u_t \quad \text{.....(2a)}$$

$$U_m = U(gs) + U(ls) = \frac{Q_G + Q_L}{A} \quad \text{..... (2b)}$$

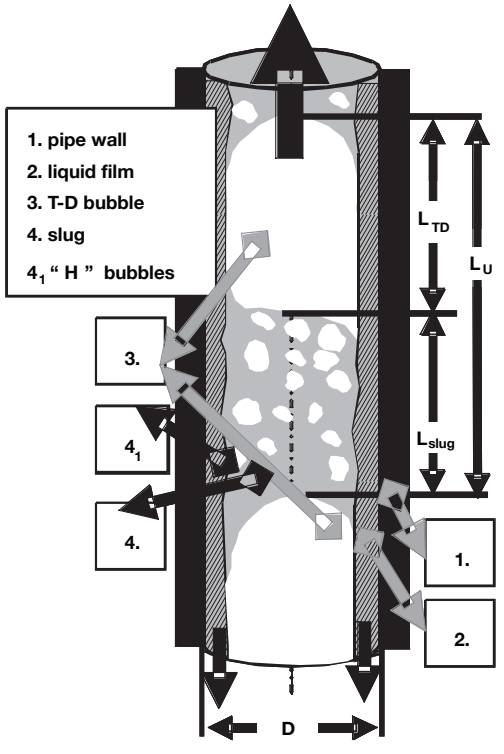

FIGURE 1: Schematic of slug flow pattern and features (observed with conventional gas lifting).

The slug flow pattern, schematically illustrated in Figure 1, is one of the most common flow patterns encountered in conventional gas lifting systems. Bubble-flow and annular flow patterns are also observed, though at much lower and extremely high gas velocities, respectively. Annular flow transport conditions are not analyzed in this paper.

The slug flow pattern (Figure 1) is generally composed of a Taylor-Dumitrescu[9] (T-D) "bullet-shape" bubble with a diameter close to the pipe diameter (a thin, downward flowing liquid film separates the bubble from the tube wall) followed by a swarm of gas bubbles in the liquid between two consecutive T-D bubbles (slug). The typical bubble populating the slug (named "Harmathy"—"H") has an ascending velocity almost independent of its size[10]. The T-D bubble and slug sub patterns repeat themselves in a statistically identical manner, as long as the fluid properties are unchanged.

Estimation of the length and void fractions of each sub-system is essential for accurate estimation of local gas-liquid density and static pressure.

Essential differences observed between conventional and SDP gas lifting are summarized as follows:

1. As the diameter of the tube is reduced to a size comparable to the equivalent diameter of the "H" bubble, the typical slug sub-pattern is first distorted, and then disappears. In tubes with D < 2.54 cm (1 in), for air-water flow at standard pressure-temperature conditions, the "H" bubbles will coalesce into slower T-D bubbles and practically disappear. In addition, the wobbling, non-spherical shape of "H" bubbles requires a pipe diameter $D >> d_H$. This condition is invalid for SDP gas lifting. Therefore, all models and calculations using conventional slug flow patterns have to be re-evaluated for SDP;
2. Conventional pipe slug flow models generally neglect the liquid film thickness, δ (as δ << D). Therefore, some models are neglecting the liquid fallback film[5] when compared to the total amount of liquid found in a slug unit. This assumption has to be re-visited for SDP;
3. For some models used to calculate the gas lifting in conventional pipes, the gas-liquid surface tension is required to assess the terminal ascending velocity of the "H" bubble, and not for calculating the liquid film flowrate;
4. A relatively strong-turbulent flow regime is associated with a conventional slug-flow pattern. The turbulent-dissipated energy[5] is responsible for breaking the tailing-edge of the T-D bubble and the formation of "H" bubbles (in the slug sub-pattern, Figure 1). For the laminar or low turbulence level in SDP, the T-D bubbles are not exposed to the breaking-coalescence process controlling the conventional slug flow pattern; and,
5. The terminal (upward) velocity, $u_{t(T-D)}$, of a T-D bubble strongly depends on the tube diameter D [Equation (3)]. With decreasing the diameter, the local gas allocation would increase with the beneficial effect of reducing gas-liquid density and, hence, the static pressure component. However, the application of the Dumitrescu[9] equation for calculating terminal velocity of a gas bubble in SDP requires further validation:

$$u_{t(TD)} \approx 1.53\sqrt{gD} \quad \text{..... (3)}$$

The Tube Diameter Effect

Ansari[5] and Hasan[6] mechanistic gas-lift models, developed for conventional diameter tubes, were extended to SDP and the results were used to observe first the effect of pipe diameter on production characteristics and then used as a baseline for assessing laboratory results with SDP. Figure 2 shows the required BHP vs. diameter for a given gas injection/liquid production rate and fixed reservoir depth; gas being injected at the bottomhole level. The

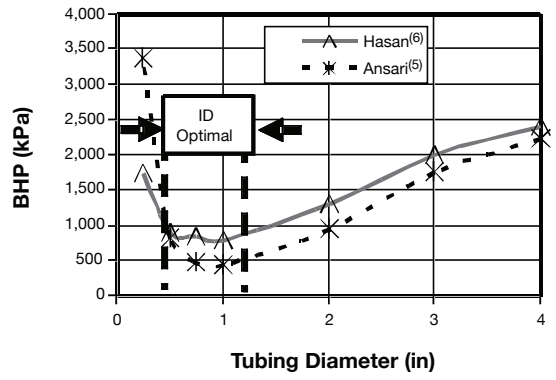

FIGURE 2: The effect of tubing diameter on the required bottomhole pressure for a production of Q_L = 1 BBD/0.16 m^3/d (H = 200 m, Q_G = 15 MCFD)—numerical model.

results using the two mentioned models (Figure 2) compare satisfactorily and suggest that, for the specified gas lifting conditions, a minimum BHP of 500 kPa (72 psia) is required (for 200 m depth, a submergence S ≈ 25% is required). Figure 2 suggests that an optimum range of pipe diameters can be calculated for a certain gas injection rate and reservoir pressure which should be exploited for producing fluids from reservoirs with low BHP.

The use of SDP for gas lift application has been previously investigated[11], however for relatively high reservoir pressure conditions only (submergence ranging from 75 – 100%). The effect of tube diameters on production under extreme low reservoir pressure conditions, and additional strategies to make it possible, is a new area. Several laboratory investigations and industrial applications using small diameter gas lift for transporting fluids over a few metres of elevation were reported[12-14]. However, no attempts have been made to assess and explain physical limitations resulting from a considerable increase of the tube length (i.e., a few hundred metres of vertical transport) to accommodate various gas-oil field applications.

Experimental Program

To investigate the effect of small pipe diameter on production performance, a laboratory experimental rig was built. Experimental results were compared to existing numerical mechanistic models and further used to develop and validate a suitable numerical model for transferring laboratory results to field depth conditions. Figure 3 is a schematic of the field and laboratory key dimension parameters for the gas lifting process. The laboratory design (Figure 3b) includes all key elements of a typical field gas-lift operation. The tube diameter is not scaled. The length of the vertical tube section (H) is approximately 3 m.

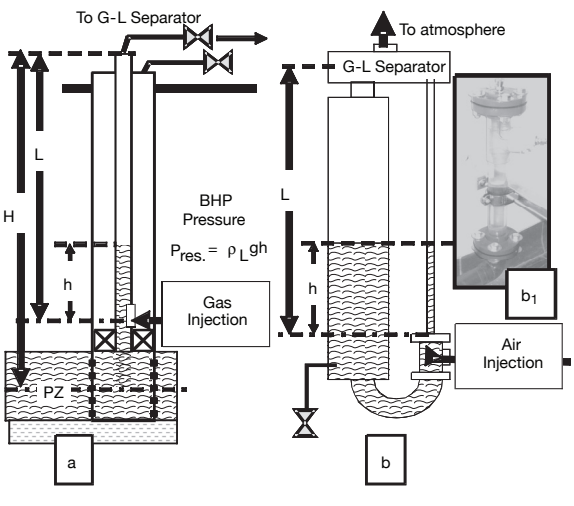

FIGURE 3: Field a) and laboratory b) schematic of one-injector gas lift key parameters—gas injector device used in the laboratory (b_1).

The laboratory experiments were designed to simulate extreme field conditions, i.e., depleted, low-pressure reservoirs. Submergence [Equation (4)—notations in Figure 3] is defined as the ratio between the distance from the injector to the liquid level to the distance from the injector to the wellhead:

$$S = \frac{h}{L} \quad \text{.....(4)}$$

The simulated reservoir pressure, P_{res}, is [Equation (5)]:

$$P_{res} = \rho g h \quad \text{.....(5)}$$

Low submergence values S < 0.25 have been used.

To assess the effect of surface tension on net liquid production, water and various concentrations of water-methanol mixtures were used. For each mixture, the surface tension was measured (room temperature).

A certain experimental run is defined by: a) tube inner diameter, D (mm); b) injected gas flow rate, Q_G (l/min); c) simulated reservoir pressure, P_{res} (as level "h" or submergence S); and, d) water-methanol concentration-surface tension.

For each run, the output measured values include: a) produced liquid rate, Q_L (litre/min)—a rotameter and a digital flow meter were used for improved flowrate measuring accuracy; b) average injection pressure, P_{in} (equivalent to BHP)—momentary and time averaged values have been recorded; and, c) maximum and minimum bottomhole pressures have been recorded over 5 min (reflecting pressure oscillation intensity). During each run, the gas injection rate was stepwise increased and then, kept constant for approximately 20 min. A digital video camera was used to record specific flow patterns for each observed gas-liquid flow regime.

Experimental Results

A summary of the experimental results used for validating a laboratory-field depth-scaling model is given in the following sections:

a) Reservoir pressures of 63.5 and 38 cm (S = 21 and 12%) were used to determine the liquid production rates for various gas injection rates with D = 12 mm (Figure 4). Figure 4 indicates that increasing the reservoir pressure (or submergence, S) by 65% (from h = 38 cm to 63 cm H_2O) at the same gas injection rate of 6 l/min enhances the liquid production rate by approximately six times (from 0.1 l/min to 0.6 l/min);

b) The onset of liquid production (CPC) for S = 21% Q_G > 4 l/min is required to initiate liquid production, and for S = 21% production is observed for Q_G > 2 l/min. The minimum gas injection rate required to initiate the liquid production (for a

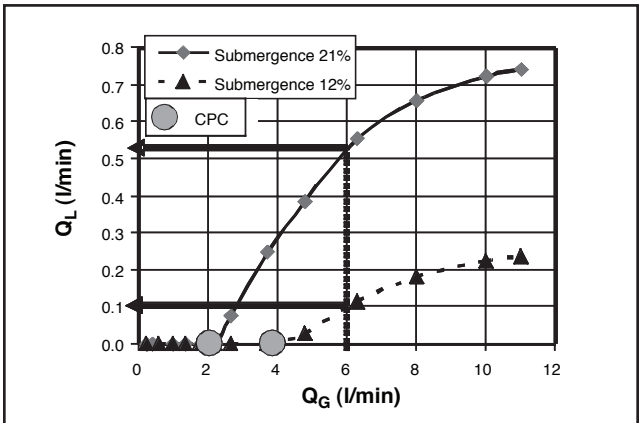

FIGURE 4: Liquid production vs. gas injected for 21% and 12% submergence (laboratory simulated reservoir pressures 63.5 and 38 cm H_2O, D = 12 mm).

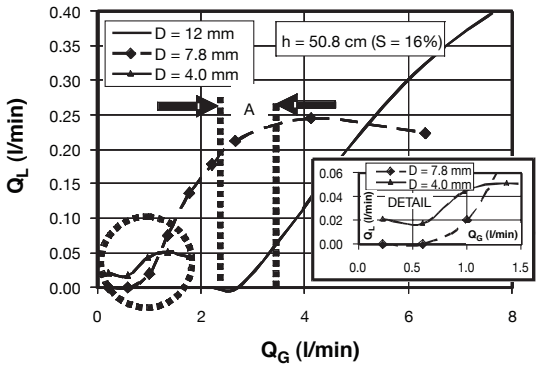

FIGURE 5: Liquid production vs. gas injection rate for 12, 7.8, and 4 mm tubes. Experiments performed at h = 50.8 cm (S = 16%).

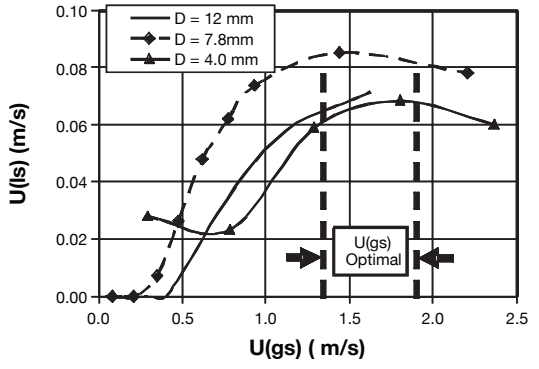

FIGURE 6: Superficial velocity of produced liquid [U(ls)] vs. [U(gs)] for 12, 7.8, and 4 mm tubes. Experiments performed at h = 50.8 cm (S = 16%).

certain reservoir pressure or submergence) is defined as "critical production conditions" (CPC).

The relative reservoir pressure or submergence [Equation (4)] required for reaching the CPC is considerably smaller (S = 12.7% for h = 38 cm) than the minimum value normally required in the conventional field operations (S = 50%)[8]. This is a result of the combined effect of a small diameter and of a much smaller depth (3 m) used in experiments as compared to the field. The liquid production results from the balance between the upward transport of gas-liquid and the liquid film fallback. It is expected that the negative effect of fallback film flow will increase with increasing well depth; and,

c) Tube diameters of 4, 7.8, and 12 mm have been used and results were compared. Figure 5 illustrates the liquid produced vs. gas injected with 4, 7.8, and 12 mm diameter tubings, and a simulated reservoir pressure of 63.5 cm H_2O (S = 21%). For $2 < Q_G < 3.5$ l/min ("A" Figure 5), the liquid production rate obtained from a 7.8 mm diameter tube exceeds the one from a 12 mm diameter pipe. At higher injection rates, 12 mm tubing indicates a higher production rate.

   The detail in Figure 5 (low Q_G) suggests that for $Q_G < 0.5$ l/min, the 4 mm tube performs better than 7.8 mm tube. For $0.5 < Q_G < 1$ l/min, performances of 4 and 7.8 mm tubes are comparable.

Figure 6 converts the actual gas-liquid rates (in Figure 5) into superficial velocities [Equations (6) and (7)]:

$$U(gs) = Q_G / A \quad (m/s) \qquad \text{.....(6)}$$

$$U(ls) = Q_G / A \quad (m/s) \qquad \text{.....(7)}$$

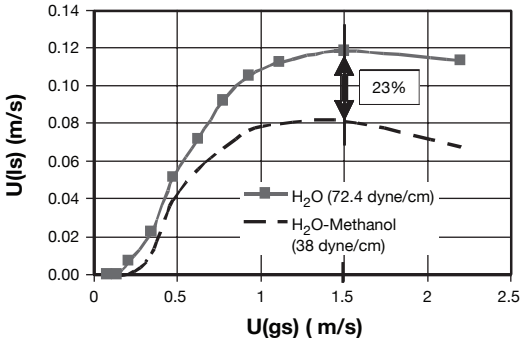

FIGURE 7: Superficial liquid velocity vs. superficial gas velocity for water only [(σ = 72.4 dyne/cm) and water-methanol (σ = 38 dyne/cm). Experiments performed at D = 12 mm, h = 63.5 cm/S = 21%].

For 1.5 < U (gs) < 2.2 m/s, a maximum range of liquid production rate is observed for all three tube diameters. Figure 6 also shows that for superficial gas velocities 1.2 < U(gs) < 1.8 m/s, the D = 7.8 mm case indicates the higher liquid production rates. However, for U(gs) > 2 m/s (and D = 4 and 7.8 mm), the superficial velocity of produced liquid declines. This is related to the increase in the frictional pressure component and its effect on total pressure drop [Equation (1)].

Regardless of whether the actual flow rates or superficial velocities are selected to display the production characteristic, a maximum productivity situation is always observed and should be exploited. This is a zone where the derivative of liquid production (or superficial liquid velocity) with respect to the sum of frictional and static pressure drops [Equation (1)] approaches zero.

d) The effect of surface tension on the liquid unloading rate was observed by changing the liquid surface tension and observing its effect on the net fluid production. The influence of film fallback rates (strong function of gas-liquid surface tension) was indirectly measured using a broad range of water-methanol mixtures (100% water to 60% water corresponding to σ = 73 to 35 dynes/cm). Figure 7 compares U(ls) vs. U(gs) (D = 12 mm, h = 63.5 cm and S = 21%) obtained with water only (σ = 72.4 dyne/cm) and water-methanol mixture (σ = 38 dyne/cm). A significant reduction of net liquid transported is observed with water-methanol experiments [23% at U(gs) = 1.5 m/s in Figure 7].

Further reduction of tubing diameter to D = 7.8 mm (at the same submergence S = 21%) acts to increasing the differences observed with D = 12 mm in Figure 7 (33% reduction at U(gs) = 1.5 m/s). The observed effect of liquid surface tension on gas lifting performances will be further used to validate an "in-house" numerical model designed to improve the present assessment of liquid fallback effect.

Visual Observations

Three specific flow patterns have been previously identified with SDP: a) (bubbly) flow formed of small, spherical "bubblets" (not to be confused with wobbling, relatively large "Harmathy's" bubbles); b) train-of-bubbles[14]; and, c) pseudo-slug (Figure 8) flow.

During the described experimental program, pseudo-slug and gas bubblets flow structures have been identified. A pseudo-slug flow pattern (Figure 8) is identified by the presence of a large ($d \approx D$, $L >> D$) bubble, (a thin fallback liquid film separates the pipe and bubble) and a small population of gas "bubblets" $d << D$ floating in the liquid separating two large bubbles (Figures 8a and 8b). It was observed that by reducing the surface tension, the population of bubblets increases. Due to their near pipe wall location and small size, bubblets are ascending at a much lower speed than the larger-sized bubbles. The "H" bubbles were not detected. Bubblets and train-of-bubble were the only flow patterns observed with 7.8 and 4 mm tubings, regardless of gas velocity and submergence level.

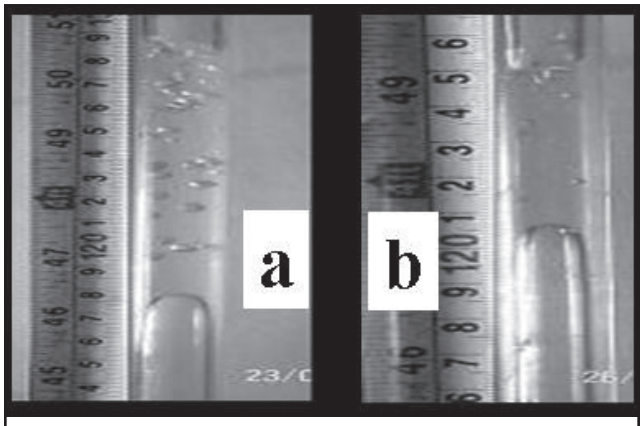

FIGURE 8: a) Pseudo slug flow pattern with water-air (D = 12 mm, h = 63.5 cm, and Ugs = 0.54 m/s): b) Train-of-bubbles with water-methanol-air (D = 7.8 mm, h = 63.5 cm, Ugs = 0.21 m/s, and σ = 38 dyne/cm).

Pressure Oscillations

Averaged injection pressure (recorded over 20 minutes of constant gas injection period) and instantaneous pressure values (maximum and minimum recorded over five minutes) were used to quantify the level of pressure-flow oscillations. For each gas flow rate and tube used, the flow instability was calculated as a ratio of the difference between maximum and minimum values of instantaneous pressures to the average injection pressure value. The per cent ratio of the maximum variation of pressure over the average pressure value was used as the indicator of the magnitude of flow instabilities (Figure 9).

Using the occurrence of pressure oscillations in excess of 10 – 20% and net production as gas-lifting criteria, three flow regimes were generally observed: a) instable stage with bubble dissipation (no net production); b) instable stage with liquid production; and, c) stable stage with liquid production. Figure 9 compares the calculated level of oscillations with production characteristic {presented as U(ls) = F[U(gs)]}. Results shown in Figure 9 suggest that the occurrence of large instabilities do not significantly affect the liquid production trend.

Numerical Modelling

A summary of the frequently used gas lift mechanistic models and their limitations as far as their applications for small diameter pipes are presented in the following section. A new model (CPC) was developed to predict depth limitations of (but not restricted to) particularly small-diameter tubings.

Gas-lift mechanistic models describe the conventional slug flow pattern (Figure 1) composed of three major sub-patterns: a) a T-D rising bubble; b) a swarm of "Harmathy" ("H")[10] type bubbles; and, c) a fallback liquid film.

By combining the "H" bubble and "T-D" bubble characteristics, and using the empirical approximation of average void fraction in the liquid slug[16], Hasan[6] developed a model to determine the average local void fraction [Equations (8a) and 8b]:

$$\alpha = \frac{L_{TD}}{L_U}\alpha_{TD} + 0.25U(gs) \quad for\ U(gs) < 0.4\ m/s \qquad \text{.....(8a)}$$

$$\alpha = \frac{L_{TD}}{L_U}\alpha_{TD} + 0.1 \quad for\ U(gs) \geq 0.4\ m/s \qquad \text{.....(8b)}$$

α_{TD} is the void fraction in the T-D bubble slug zone unit [Equation (9)]:

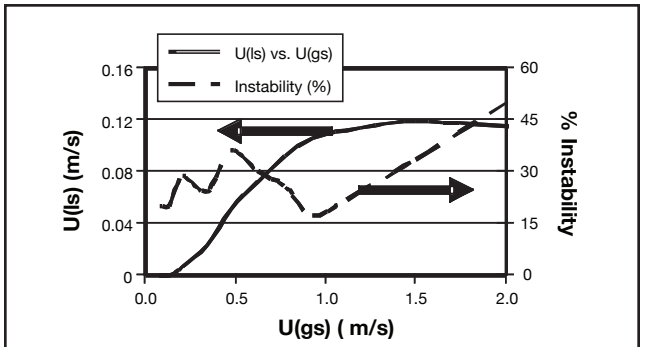

FIGURE 9: Flow instability and liquid-gas superficial velocities (D = 7.8 and h = 63.5 cm).

$$\alpha_{TD} = \frac{U(gs)}{U_G} = \frac{U(gs)}{cU_m + U_{t(TD)}} \qquad \text{.....(9)}$$

Equation (10) calculates the terminal velocities of T-D bubble[9] mainly as a function of pipe diameter, D:

$$U_{t(TD)} = 0.35\sqrt{gD\left(\frac{\rho_L - \rho_G}{\rho_L}\right)} \qquad \text{.....(10)}$$

Hasan's model[6] considers the gas-liquid slip, but ignores the effect of fallback film (usually negligible for conventional tubing slug/gas-lift and moderate gas/liquid ratios).

Ansari's model[5] considers the slip between the phases as well as the effect of fallback film as being independent to interfacial tension by calculating the velocity U_{LTB} of downward falling liquid film as (Brotz[17]):

$$U_{LTB} = \sqrt{196.7 g \delta_L} \qquad \text{.....(11)}$$

where the average film thickness, δ_L, is:

$$\delta_L = \frac{D}{2}\left(1 - \sqrt{\alpha_{TD}}\right) \qquad \text{.....(12)}$$

Visual observations performed during this study as well as previous investigations using SDP indicate that "H" bubbles cannot develop.

However, both Ansari[5] and Hasan[6] models were used to compare experimental results.

Figure 10 compares experimental and model[5] data (for D = 12 mm, H = 3 m, and h = 63.5 cm/S = 20%). For indicated gas lift conditions, Hasan's model[6] failed to predict any net production, therefore it is not included.

Ansari's model underestimates the liquid production rates by about 60% (Figure 10). Another observation is related to the critical production condition (CPC is defined as the minimum gas injection rate required for initiating the liquid production). Ansari's model predicts the onset of the liquid production at a superficial gas velocity of 0.75 m/s. However, the measured gas superficial velocity corresponding to the CPC was 0.4 m/s. Ansari's model, therefore, overpredicts the gas injection rate corresponding to CPC by about 80%.

Comparison of the experimental and model data suggests that there is a need for a model capable of accurately predicting and scaling (e.g., H > 50 m) laboratory results with SDP to field depth. A new model, aiming at a better evaluation of critical production conditions, was developed.

The critical production conditions (CPC) model was developed as a simplified tool for estimating potential candidates for SDP gas lift technologies.

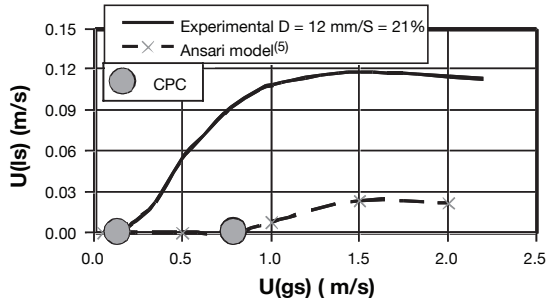

FIGURE 10: Superficial velocity of liquid vs. gas-laboratory data and model prediction (water only, D = 12 mm, h = 63.5 cm/S = 21%).

The balance between the reservoir pressure and integrated frictional-static pressures [Equation (13)] is used. The local void fraction assumes a linear development, reaching a 100% (no liquid) condition at the wellhead (CPC condition).

$$P_{res} = \sum_{H=0}^{H} \left[(dP)_{st} + (dP)_{fr} \right] \quad \text{..... (13)}$$

Equations (14) and (15) are used to estimate frictional and static pressure drops:

$$(dP)_{fr} = f_M \frac{\rho_m U_m^2}{2D} (L+h) \quad \text{..... (14)}$$

$$(dP)_{st} = \rho_m g (L+h) \quad \text{..... (15)}$$

where the local two-phase density, ρ_m, is calculated by using the local void fraction, α, in Equation (16):

$$\rho_m = \bar{\alpha}\rho_G + (1-\bar{\alpha})\rho_L \quad \text{..... (16)}$$

By combining Equations (13), (14), (15), and (16), the void fraction [Equation (17)], which satisfies the pressure balance, is:

$$\bar{\alpha} = \frac{\rho_1}{\rho_1 - \rho_G} \left[1 - \frac{gh}{L\left(g + f_M \frac{U_m^2}{2D} \right)} \right] \quad \text{..... (17)}$$

The liquid film thickness is given by Equation (18)[15]:

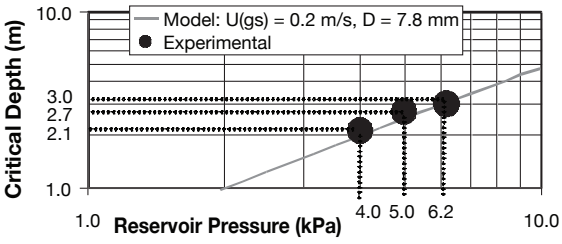

FIGURE 11: Critical depth vs. reservoir pressure [The "CPC" model prediction versus laboratory-measured values at D = 7.8 mm and U(gs) = 0.234 m/s].

$$\delta = 0.32D(3Ca)^{2/3} \quad \text{..... (18)}$$

where Ca is the capillary number:

$$Ca = \frac{\mu U_{film}}{\sigma} \quad \text{..... (19)}$$

Equations (18) and (19) are used to calculate the thickness of the downward flowing film as a function of surface tension and viscosity. The wavy film interface effect was not considered.

At the CPC condition, a linear variation of the void fraction was assumed between the injection and production levels (WH).

The CPC model was first used to assess the effect of tube length (well depth) for various tube diameters and reservoir pressure and to determine the minimum required gas injection rate at the CPC (the moment a net liquid production is recorded). The model was validated by using the laboratory data.

CPC model validation was performed using the laboratory data obtained from gas lifting experiments using 7.8 mm and 12 mm diameter tubes.

The first set of experiments used for CPC model validation was conducted by using 7.8 mm diameter tube with a specific gas injection rate of 0.206 m/s. The three experimental data points shown in Figure 11 were measured at water column heights of 38.1, 50.8, and 63.5 cm (corresponding to reservoir pressures of 4, 5, and 6.2 kPa, respectively). Predicted values of critical depth (i.e., maximum possible depth the well can produce at a certain gas injection rate) agree reasonably well with the laboratory-measured values.

The second group of experiments used for model validation was conducted by using 12 mm diameter tube and U(gs) = 0.316 m/s and 0.707 m/sec (Figure 12). The critical depth assessed for the CPC model also agreed well with laboratory experimental data (for a reservoir pressure of 3.7 kPa and U(gs) = 0.326 m/s, a critical depth of 2.1 m is predicted; the measured critical depth for this case was 1.81 m, indicating a 14% error). The maximum difference recorded between measured and calculated values of critical depth for ten different conditions was less than 18%.

Further to additional validation of the CPC model within laboratory depth conditions (Figure 12), the critical depth conditions for field (depth) scale was predicted using a linear extrapolation in the depth-pressure diagram using log-log co-ordinates (Figure 12). The linear feature (in the log-log diagram) has been observed using a large number of laboratory data. Figure 12 suggests that for a reservoir pressure of 400 kPa, a critical depth of approximately 300 m is required [for D = 12 mm and U(gs) of 0.3 to 0.7 m/s]. The submergence required at the CPC condition is 13%.

For practical reasons, a reservoir pressure exceeding the critical depth limit indicated by the CPC model by 25 to 30% is required for achieving a net gas lift upward transport [for given D and U(gs)].

The CPC model is used in Figure 13 to compare critical depth calculated for P_{res} = 400 kPa at superficial gas velocities between 0-3 m/s for D = 7.8, 12, and 25 mm. For U(gs) < 1.5 m/s, it

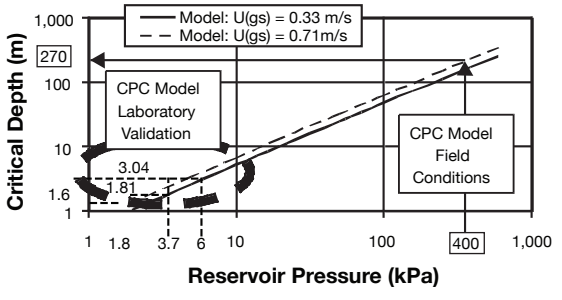

FIGURE 12: Critical depth vs. reservoir pressure ("CPC" Model validations and field predictions for D = 12 mm, U(gs) = 0.33, and 0.71 m/s).

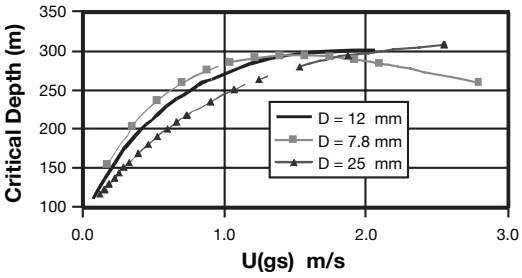

FIGURE 13: Critical depths vs. superficial gas velocity for D = 7.8, 12, and 25 mm (reservoir pressure 400 kPa/58 psi).

appears that D = 7.8 mm is advantageous. However, if U(gs) > 1.7 m/s, a larger diameter will perform better, mainly because of increasing the frictional pressure drop. Also, it should be noted that the benefit of using 7.8 mm tubing as opposed to 12 mm tubing is not significant. For practical purposes, using 12 mm tubing may be preferable.

Future Work

In order to improve the understanding on the effects of liquid film fallback and extend the model from limiting threshold production estimations to calculations of an actual production situation, additional laboratory work needs to be performed. Additional laboratory work and field testing using SDP and conventional tubing for gas lifting operating under low reservoir pressure conditions are also required.

Conclusions

1. Experimental and numerical modelling studies have been conducted to investigate advantages and limitations of using small-diameter tubes for unloading liquids from gas wells with very low reservoir pressure.
2. Replacing conventional diameter tubing (D > 1 in) with SDP (D < 1 in) offers potential advantages for unloading water and resuming production from gas wells with low reservoir pressure.
3. An experimental apparatus was designed and operated to produce salient proof of the concept of gas lifting using SDP. Experimental data have been further used to validate a model developed to assess critical depth considered for field applications.
4. The new CPC mechanistic model evaluates the effect of liquid film fallback observed for conventional and SDP gas lift operations better than existing gas lift models, making it suitable for estimating the potential application of SDP in low pressure reservoirs. Laboratory validation of the new (CPC) model indicates a range of errors under 18%.
5. Laboratory tests were able to identify and quantify the occurrence of flow instabilities reflected through significant oscillations of total (static and dynamic) transport pressure. It appears that instabilities do not negatively affect average liquid production.

Acknowledgements

The authors would like to acknowledge the support and technical input of Mr. Ray Ivey, Dr. A. Babchin, and Dr. A. Turta for valuable discussions and suggestions regarding the physics of liquid film and gas lifting, Mr. Sean Watt for contributions in designing and building of the experimental set-up, and the IRAP – NRC-CNRC program and P. R. Toma Consulting Ltd. for the support given to this project during 2003 – 2004, as well as permission to publish.

NOMENCLATURE

BHP	=	bottomhole pressure
c	=	velocity distribution coefficient [Equations (2) and (9)] usually c = 1.2
CPC	=	critical production condition
D	=	tubing diameter (ID) (mm)
f_M	=	Moody friction factor
g	=	acceleration of gravity (m/s^2)
A	=	cross-section of tube [Equations (2b), (6a), and (6b)] (m^2)
h	=	liquid column height/shut-in reservoir pressure (Figure 3) (m)
H	=	depth perforation-WH (Figure 3a)
IPR	=	inflow production relationship [BHP = F(Q)]
L	=	WH-gas injection length (Figure 3) (m)
L_{TD}	=	Taylor-Dumitrescu bubble length (Figure 1)
L_{slug}	=	slug sub-pattern length (Figure 1)
L_u	=	slug unit length (Figure 1)
P	=	pressure (kPa) (1 psi = 6.895 kPa)
P_{res}	=	reservoir pressure (kPa)
dP_{st}	=	static pressure loss (kPa)
dP_{fr}	=	frictional pressure loss (kPa)
Q_G	=	gas flow rate (l/min)
Q_L	=	liquid flow rate, (l/min)
S	=	submergence [Equation (4)] (–) or (%)
SDP	=	small diameter pipes (D <1 inch)
T-D	=	"Taylor-Dumitrescu" bubble [see terminal velocity Equations (3) and (10)]
H	=	"Harmathy" bubble
U(gs)	=	superficial gas velocity [Equation (6a)] (m/s)
U(ls)	=	superficial liquid velocity [Equation (6b)] (m/s)
Um	=	gas and liquid transport velocity U(gs)+U(ls) (m/s)
U_G	=	(actual) gas velocity (m/s)
U_{LTB}	=	fallback liquid film velocity [Equation (11)] (m/s)
U_{film}	=	average liquid film velocity [Equation (19)] (m/s)
u_t	=	bubble terminal velocity (m/s)
VLP	=	vertical lift performance [P = F(Q)]
WH	=	wellhead

Greek Symbols

α	=	void fraction [Equation (9)] (–)
α_{TD}	=	void fraction in the T-D sub-pattern
δ_L	=	liquid film thickness (m)
ρ_L	=	density of liquid phase (kg/m^3)
ρ_G	=	density of gas phase (kg/m^3)
ρ_m	=	density of the mixture (kg/m^3)
σ	=	surface tension [N/m = (Dyne/cm)/1,000]

REFERENCES

1. EICHER, H.V., Jr., The History of Gas Lift and Its Modern Application to the Petroleum Industry; *The Petroleum Engineering Journal, January 1952.*
2. BROWN, E.K., Overview of Artificial Lift Systems; *Journal of Petroleum Technology, pp. 2384-2396, October 1982.*
3. GOVIER, G.W. and AZIZ, K., The Flow of Complex Mixtures in Pipes; *Van Nostrand Reinhold, New York, 1972.*
4. BRILL, J.P. and MUKHERJEE, H., Multiphase Flow in Wells; *SPE Monograph Series, Vol. 17, 1999.*

5. ANSARI, A.M., SILVESTRE, N.D., SARICA, C., SHOHAM, O., and BRILL, J.P., A Comprehensive Mechanistic Model for Upward Two-Phase Flow in Wellbores; *paper SPE 20630, SPE Production and Facilities, pp. 143-151, May 1994.*
6. HASAN, A.R., Void Fraction in Bubbly and Slug Flow in Downward Vertical and Inclined Systems; *paper SPE 26522, SPE Production and Facilities, pp. 172-176, August 1995.*
7. NICKLIN, D.J., WILKES, J.O., and DAVIDSON, J.F., Two-Phase Flow in Vertical Tubes; *Transactions of the Institution of Chemical Engineers, Vol. 40, p. 61, 1962.*
8. TOMA, P., LANDRY, B., SCHUBERT, L., and MILLER, C., Field Results of Waterflood Enhancement Using a Gas Lifting Strategy; *paper 96-32, presented at 47th Meeting of the Petroleum Society, Calgary, AB, June 1996.*
9. DUMITRESCU, D.T., Stromung an einer Luftblase im senkrechten Rohr, z. Angew; *Math. Mech. Vol. 23, No. 3, pp. 139-149, June 1943.*
10. HARMATHY, T.Z., Velocity of Large Drops and Bubbles in Media of Infinite or Restricted Extent; *American Institute of Chemical Engineers Journal, Vol. 6, No. 2, pp. 281-288, June 1960.*
11. THRASH, P.J., What About Gas Lifting Tubingless Completions?; *The Petroleum Engineer, pp. 33-36, September 1960.*
12. REINEMANN, D.J., PARLANGE, J.Y., and TIMMMONS, M.B., Theory of Small-Diameter Airlift Pumps; *International Journal of Multiphase Flow, Vol. 16, No. 1, pp. 112-122, 1990.*
13. DE CACHARD, F. and DELHAYE, J.M., A Slug-Churn Flow Model for Small-Diameter Air Lift Pumps; *International Journal of Multiphase Flow, Vol. 22, No. 4, pp. 627-649, 1996.*
14. BERGLES, A.E., COLLIER, J.G., DELHAYE, J.M., HEWITT, G.F., and MAYONGER, F., Two-Phase Flow and Heat Transfer in the Power and Process Industries; *Hemisphere, Washington, McGraw-Hill, Chapter 1, pp. 6-12, 1981.*
15. STARK, J. and MANGA, M., The Motion of Long Bubbles in a Network of Tubes; *Transport in Porous Media, No. 40, pp. 201-218, 2000.*
16. AKAGAWA, K. and SAKAGUCHI, T., Fluctuation of Void Fraction in Two-Phase Flow; *JSME Bulletin, Vol. 9, p. 104, 1966.*
17. BROTZ, W., Uber die Vorausberechnung der Absorptionsgesch-windingkeit con Gasen in Stromenden Flussigkeitsschichten; *Chemie Ingenieur Technik, No. 26, p. 470, 1954.*

Provenance—Small-Diameter Gas Lift Systems—A Potential Technical Solution for Transport of Fluids From Low-Pressure Reservoirs (2004-104), first presented at the 5th Canadian International Petroleum Conference (the 55th Annual Technical Meeting of the Petroleum Society), June 8 - 10, 2004, in Calgary, Alberta. Abstract submitted for review December 2, 2003; editorial comments sent to the author(s) August 26, 2005; revised manuscript received September 20, 2005; paper approved for prepress September 20, 2005; final approval May 11, 2006.

Authors' Biographies

Javier Becaria is an enhanced gas recovery specialist with EnCana Corporation in Calgary, Alberta. He obtained a MS in petroleum engineering from the University of Alberta, where he conducted research on multiphase flow in pipes. He obtained his engineering degree in petroleum engineering from the Universidad Industrial de Santander, Colombia in 1977, and worked as laboratory supervisor and field engineer for Halliburton, Latin America during 1997 – 2002. His research topics of special interest are: multiphase flow in pipes, formation damage, drilling mud, and environmental-related topics. Javier Becaria has a P.Eng. designation and is a member of the Petroleum Society. (becariaj@yahoo.com.ar)

Peter Toma is director of P.R Toma Consulting Ltd. and an adjunct professor with the University of Alberta. He is a distinguished scientist (in residence) with The Alberta Research Council where, during the last 28 years, he has been conducting industry-related R&D projects in the area of multiphase flow and heat transfer, flow assurance, metering, and transportation for conventional and heavy oil and gas production systems. During his 45 years of engineering and R&D activities, he was instrumental in developing, testing, and moving to manufacture and field new technologies and new products. Peter Toma has a Ph.D. and a P.Eng. designation, as well as being an ASME fellow. (ptoma@telus.net)

Ergun Kuru is an associate professor of petroleum engineering at the University of Alberta. He received a B.Sc. degree from the Middle East Technical University, and M.Sc. and Ph.D. degrees from Louisiana State University, all in petroleum engineering. His research interests include drilling optimization, underbalanced drilling, cuttings transport, and formation damage. Dr. Kuru is a member of SPE and the Petroleum Society. Dr. Kuru is an associate technical editor of the ASME Journal of Energy Resources Technology and a member of SPE's continuing education committee.